EXTRACTION OF IMPERVIOUS SURFACE AREA USING ORTHOPHOTOS IN RHODE ISLAND

Yuyu Zhou
Y. Q. Wang
Department of Natural Resources Science
University of Rhode Island
Kingston, RI 02881
ilikespoon@mail.uri.edu
yqwang@uri.edu

ABSTRACT

Suburban sprawl has been identified as the most important social and environmental issue facing Americans in their community. Suburban development consumes green space, widens urban fringes, increases impervious surface areas (ISA), and puts pressure on environmentally sensitive inland and coastal areas. Urban runoff, mostly through ISA, is the leading source of pollution in the Nation's estuaries, lakes, and rivers. ISA can serve as a key environmental indicator due to its impacts on water systems and its role in transportation and concentration of pollutants. Quantifying precise spatial locations and distributions of ISA has become increasingly important with growing concern over water quality in this country. Classification of high spatial resolution remote sensing data is an important method to obtain ISA information. In this study we used 1-meter spatial resolution true color digital aerial photography data for extracting ISA information in the coastal Rhode Island. We developed a synthetic algorithm based on the multiple agent segmentation and classification. In this algorithm, the indices describing shape feature of objects were introduced in multiple agent segmentation. The shadow problem that is common in high spatial resolution remote sensing images has also been considered. Existing GIS data were used in the classification and post-classification process. The testing result indicates that this synthetic algorithm performs well in obtaining precise ISA areas and the result is better than that from pixel-based classification.

INTRODUCTION

Impervious surface area (ISA) is defined as any impenetrable material that prevents infiltration of water into the soil. Urban pavements, such as rooftops, roads, sidewalks, parking lots, driveways and other manmade concrete surfaces, are among impervious surface types that featured the urban and suburban landscape. ISA has been considered as a key environmental indicator due to its impacts on water systems and its role in transportation and concentration of pollutants (Arnold and Gibbons, 1996). ISA has also been recognized as an indicator of intensity of urban environment. With advent of urban sprawl ISA has been identified as a key issue in habit health (Brabec *et al*., 2002). Quantification of the percentage of impervious surface in landscape has become increasingly important with growing concern of its impact on the environment (Civco *et al*., 2002; Wang and Zhang, 2004; Weng, 2001; Dougherty *et al*., 2004).

As a result of urban land development, coastal state of Rhode Island experiences the problems caused by urban runoffs. However, there is lack of information on high spatial resolution ISA in the state. A previous study using Landsat remote sensing data revealed the increasing urban land-use and land-cover but not be able to obtain precise ISA coverage with 30-meter pixel size (Novak and Wang, 2004).

Conventionally, manual delineation through aerial photography has been used to extract accurate ISA information (Draper and Rao, 1986). For example, the currently available land-use and land-cover data for the state were developed based on manual interpretation of 1987 and 1995 aerial photography data, respectively. However, manual delineation is labor-intensive, prohibitively expensive for large area, and difficult to keep the interpretation results consistent. In addition, ISA is not a separate class in general purpose land-use and land-cover maps. ISA can be obtained from classification of remote sensing data. Due to limitations of spectral mixing and spatial resolutions, the accuracy of ISA extraction has always been challenged through classification process. Therefore, efforts have been made to extract ISA from a variety of remote sensing data sources and through modeling. For example, sub-pixel methods have been developed for urban land classification (Lu and Weng, 2004). Wang and Zhang (2004)

developed a SPLIT model to extract ISA information through sub-pixel extraction by integration of Landsat TM and high spatial resolution digital multispectral videography data. Although this method is capable of extracting the percentage of ISA in mixed pixels, it is difficult to obtain a precise spatial distribution and coverage of ISA as needed. Estimations of ISA through land-use and land-cover data and impervious surface coefficient have been used by the U.S. Environmental Protection Agency (EPA) and other researchers (Jennings *et al.*, 2004; Sleavin *et al.*, 2000). The coefficient is produced using truth GIS data or high spatial resolution remote sensing data in combination with land-use and land-cover data. This method is applicable for the areas that have coarse or middle spatial resolution GIS data and has been tested and applied in the Mid-Atlantic region or the EPA Region 3 (Jennings *et al.*, 2004). The difficulty of using this method is that the coefficient has to be established and validated for different study areas. Also the same challenge of precise coverage and accurate location of ISA remains. Therefore extraction of ISA from high spatial resolution remote sensing data in meter or sub-meter level is in demand particularly by the planning agencies.

The conventional pixel-based methods will produce more dramatic salt-and-pepper effect due to the increased spatial resolution and noise level. Furthermore, the spatial information such as neighborhood, proximity and homogeneity can not be used sufficiently in these methods (Burnett and Blaschke, 2003). To conquer these problems and make sufficient use of spatial information from high spatial resolution data object-based classification has been developed (Baatz and Schäpe, 2000; Shackelford and Davis, 2003). Object-based methods simulate the process of human image understanding in feature extraction. It is especially suitable for processing high spatial resolution images. In addition, other spatial information can be integrated in modeling process. Object-based methods have been used in classification of high spatial resolution images and the change detection (Blascheke and Strobl, 2001; Walter, 2004). The commercial software, such as eCoginition (@ Definiens Imaging, Germany), is among the first object-based systems, and has been used for classification of high spatial resolution images (Wang *et al*., 2004). Hay *et al*. (2003) compared three image-object techniques, *i.e.*, Fractal Net Evolution Approach, Linear Scale-Space, and Multiscale Object-Specific Analysis, for analysis of landscape structure.

An important step for object-based classification is to define regions in an image corresponding to objects in a ground scene. Successful image segmentation is the most important prerequisite (Baatz and Schäpe, 2000). Burnett & Blaschke (2003) discussed the application of multi-scale segmentation in landscape analysis. Plenty of algorithms of segmentation available with various pros and cons, such as texture segmentation, watershed transformation and mean shift have been developed in the past (Woodcock and Harward, 1992; Li *et al*., 1999; Comanicu and Meer, 2002; Hu *et al*., 2005), and Blaschke *et al* (2004) have a recent overview on image segmentation. Meinel and Neubert (2004) compared and evaluated the segmentation results from high resolution satellite imagery using several programs (eCognition, InfoPACK and CAESAR). As pointed by Baatz and Schäpe (2000), few of those methods lead to qualitatively convincing results that are robust and under operational setting applicable. Some of the methods are difficult for practical application because of the computing speed or the accuracy (Woodcock and Harward, 1992). Woodcock and Harward (1992) developed a multiple pass algorithm to extract forest information from Landsat TM data. This algorithm improved the segmentation of images from scenes better modeled as a nested hierarchy and achieved reasonable accuracies with the consideration of local best fitting and merging coefficient. However, this algorithm was developed to process remote sensing data at 30-m spatial resolution. Further modification is necessary when dealing with high spatial resolution remote sensing imagery at meter or sub-meter levels. For example for high spatial resolution imagery, the shape information is an important measure in image segmentation and object-based classification, but it was not considered in the multiple-pass algorithm.

The classifiers such as fuzzy logic, minimum distance, and maximum likelihood used in the pixel-based classification can still be used in object-based methods. For example fuzzy logic used in pixel-based methods is commonly used in the object-based classfication (eCognition User Guide, 2004; Shackelford and Davis, 2003; Benz *et al.*, 2004). In order to use fuzzy logic, a rule-base must be established first. Subjective factors will be included in the process. Maximum likelihood classifier may be a better one and more useful when prior knowledge is available and statistic criteria should be taken into account.

In this paper we developed a new synthetic algorithm by incorporating shape information and prior knowledge for the extraction of ISA. The added shape information enhanced the multiple pass segmentation and the prior likelihood knowledge of urban land cover improved the classification. With GIS supported post-classification process a precise ISA extraction was achieved from high spatial resolution remote sensing data. This allows us to modernize and enhance the existing GIS and add new ISA data for the statewide GIS system known as RIGIS, and to demonstrate a model that can be replicated for statistical and graphic comparison of ISA data from high spatial resolution remote sensing data.

METHOD

Data Sources and Process

We selected a subset of Narragansett in the east coast of the state as a test area (Fig. 1a). This is a typical suburban community with intensive urban development. Residential and commercial areas are the representative landscape. ISA is a major concern of the community in terms of watershed management and environmental monitoring. The Statewide Planning Program is pursuing different methodologies and data sources such as true-color digital orthophoto data to extract precise ISA information for the state. The true color orthophoto data set was acquired in July 19, 2003 by the Rhode Island Statewide Planning Program through the National Agricultural Imagery Program (NAIP). This 1-meter ground sample distance ortho imagery has a horizontal accuracy of within +/-3 meters of reference digital ortho quarter quads (DOQQS) from the National Digital Ortho Program (NDOP). The ortho images are projected into Rhode Island State Plane Coordinate System with zone 3800 in U.S. Survey feet by Rhode Island GIS. The resulting resolution in this coordinate system is 1 meter (3.28 feet). The data set has red, green and blue bands and distributed in GeoTIFF format (Fig. 1b). We tested our algorithm using a subset of the true color orthophoto data.

Texture information is helpful for the definition of regions that have different levels of internal variance (Woodcock and Harward, 1992). We used a 3 x 3 window on the true color digital orthophoto to extract the texture information as one of the features in the segmentation process. We focused on two categories of ISA and none-ISA only for the classification process. Finally, the developed algorithm was applied in the Rhode Island.

Multiple Agent Segmentation

We modified the multi-pass algorithm to accommodate the use of the high spatial resolution imageries. Figure 2 illustrates the technical flow of the synthetic algorithm. We developed a segmentation submodel (Fig. 2a) that incorporated the shape information by heterogeneity change in place of spectral difference as the cost function for merging the regions. In the original multiple-pass algorithm, decision to merge two regions is based on the distance of channels in spectral space. In this study we used change of heterogeneity, *i.e.*, combination of shape, spectral and texture information to determine the merge of two regions. There are different possibilities to describe the change of heterogeneity before and after a merge. A common method for heterogeneity change, such as the one used by eCognition, is as follows.

The overall heterogeneity change h_{change} includes spectral, texture and shape agents.

$$h_{change} = \sum_{A=1}^{m+1+2} w_A (n_{obj1} \cdot (h_{A,m} - h_{A,obj1}) + n_{obj2} \cdot (h_{A,m} - h_{A,obj2})) \quad (1)$$

where h_{change} is the overall change of heterogeneity when two regions are merged; $h_{A,m}$ is a heterogeneity of the merged region for the agent *A*; $h_{A,obj1}$ and $h_{A,obj2}$ are the heterogeneities for two regions being merged for the agent *A*; n_{obj1} and n_{obj2} are the number of pixels in each of the two regions being merged; and w_A is the weight for each heterogeneity measure for the agent *A* (eCognition User Guide, 2004; Shackelford and Davis, 2003).

In this study, we defined six agents for the *A*. We used three spectral channels from the true color orthophoto as *A=1, 2, 3 (i.e., m=3)* for the heterogeneity measures described in *Eq. (1).* We used the 4th channel (*A=4*) for the texture component, and the 5th and 6th channels (*A=5, 6*) for the shape components.

The multiple pass algorithm can produce segmentations with minimal error by allowing merging to occur. In this merging process at least spectral average heterogeneity of all image objects will increase. An image region is merged with the adjacent image region to produce minimum increase of heterogeneity. As for the adjacent regions, we adopted a 4-way method tested by Woodcock and Harward (1992).

In the segmentation submodel, the merge process starts from single pixel objects and merges the small objects pairwise into larger ones. The ideal algorithm for a heterogeneity change metric $\Delta h(obj_1,obj_2)$ for two regions and the 4-way definition of adjacent regions can be stated as follows.

Stage 1. Initially, each pixel forms a region R_i, $1<i<N_{pix}$, in image space. Let R be the set of all such regions. N_{pix} represents the number of pixels in the image.

Stage K. At the k_{th} stage of the segmentation, the regions remaining after the $k\text{-}1_{th}$ stage begin to merge. The heterogeneity change between all remaining adjacent regions, R_i and R_j, $\Delta h(obj_i,obj_j)$, $i<j$, is calculated and this list is ordered so that the minimum heterogeneity change, $\Delta h(obj_a,obj_b)$, between regions R_a and R_b is determined. If this minimum heterogeneity change is less than the global threshold, then regions R_a and R_b are merged, and R_b is replaced by R_a in R.

Stage Final. This is the stage where no heterogeneity change for pair of adjacent regions is less than global threshold. The algorithm then stops, and the regions remaining in set R form the resulting segmentation.

One merge per stage is allowed in order to avoid the error. However, the computing time is an important consideration for high spatial resolution remote sensing images. The multiple pass algorithm allows multiple merges per pass to minimize both the computing time per pass and the overall number of passes and keeps a minimum error of merging at the same time. In order to minimize the merging error and to improve the merging efficiency, two techniques were introduced, *i.e.*, local mutual best fitting and merge coefficient (C_m) (Woodcock and Harward, 1992). For local mutual best fitting, the following conditions under which two regions were allowed to merge on any given pass were specified. 1) Neither region has previously merged on this pass; 2) heterogeneity change between the regions must less than the threshold; and 3) each region must be a nearest neighbor of the other. The merge coefficient is used to calculate a new threshold for each pass. If n_{reg} represents the current number of regions, the smallest heterogeneity changes for all n_{reg} regions are calculated and ordered. The new histogram threshold (T_h) which is the heterogeneity change below which $C_m \times n_{reg}$ ordered heterogeneities change lie. Therefore, there are two thresholds: global threshold (T_g) and T_h. The pass threshold (T_p) is defined as the minimum of T_g and T_h (Woodcock and Harward, 1992).

The main parameters used in this experiment are that the T_g for the entire image is 2000; the C_m is 0.95; w_q for spectral and shape components are 0.8 and 0.2, respectively. This same parameter set is also used in the whole Rhode Island.

The multiple pass algorithm has difficulty to differentiate shadow covered ISA and tree crowns. The shadows caused by tall vertical objects such as tree crowns are unavoidably associated with high spatial resolution imageries. The tree crowns and shadows are always connected, overlapped, and hold insignificant spectral difference among them (Fig. 3a). The multi-pass algorithm could not separate the tree crown and the ISA covered by the crown shadow (Fig. 3b). Therefore, we used a further split-and-merge method for those types of mixed regions. The procedures of a shadow-effect submodel are illustrated in Figure 2b. First, the mixed regions are identified based on the spectral feature of these regions. Those mixed regions are separated into single pixels and then the multiple pass algorithm is applied. The global threshold for this new segmentation is assigned small value. The trees crowns and the shadows were segmented and the separated regions were identified (Fig. 3c). Finally, the process of region constraint in the multiple pass algorithm was applied in the segmentation. In this study the T_g for shadow-effect submodel was 80.

Classification and Post-classification Process

A successfully segmented image was obtained after the initial and additional segmentation processes. The next step was to assign a class label to each of the regions on segmented image through a classification process. This process is shown in Figure 2c as the classification submodel. We used the maximum likelihood classifier on the segmented image in which prior knowledge of ISA from available information sources of GIS data and remote sensing derived classification results could be adopted.

For the object-based method, there is variability in each object candidate. Therefore, in this study the variability of classes was taken into account by using the maximum likelihood and statistical criteria expressed using covariance matrix was utilized in the classification.

After the training samples were selected for certain land cover types the maximum likelihood classification was performed to obtain the primary ISA coverage. We then used the ratio of the border length of the regions classified as shadow that are adjacent to impervious surface areas with all the border length to separate shadow covered ISA and other land cover types. This ratio varies with the sun azimuth and elevation angles. We derived the threshold for this ratio from a series tests across the mapping areas.

Upon finishing the classification we used the existing GIS data through a post-classification to extract ISA that was still not be identified through the process. For example, some of the road segments are completely covered by

tree crowns and impossible to be separated on high spatial resolution imagery since the ISA information does not exist. We used a rasterized GIS transportation data as a reference to identify the road networks and integrated the road data with output from the classification submodel to obtain the final ISA coverage (Fig. 2d). The post-classification warrants that the connected ISA is not interrupted and the final result represents the best information from both high spatial resolution remote sensing and GIS data.

RESULTS

Figure 4 illustrates the ISA extracted by different methodologies for the test area. Visual comparison of the classification results reveals the differences between ISA from pixel-based algorithm and our synthetic algorithm. Conventional pixel-based classification shows the salt-and-pepper effect in the test area (Fig.4a) and an enlarged subset (Fig.4b). Our synthetic algorithm treated groups of pixels as the classification targets and achieved more patchy and connected ISA coverage (Fig.4c and 4d).

Because of the difference between object-based and pixel-based method, different accuracy assessments are used in previous research. Herold *et al.* (2002) used the accuracy assessment based on objects, while Shackelford and Davis (2003) and Wang *et al.* (2004) used random points based accuracy assessment. We used accuracy assessment based the random points to check the accuracy of the classifications for the comparison between different classification methods. We selected 100 samples randomly and evenly split among the ISA and none-ISA categories from the test area. We examined the classification accuracies for the two categories only. The confusion matrix indicates that the pixel-based classification achieved 88% overall accuracy for ISA (Table 1). The producer's and user's accuracies are 91.3% and 84% for the ISA, and 85.2% and 92% for the None-ISA. The Kappa coefficient is 0.76. The synthetic algorithm achieved a 93% overall accuracy for ISA (Table 2). The producer accuracies are 93.9% and 92.2% for ISA and none-ISA categories. The user accuracies are 92% and 94%, respectively, with a 0.86 Kappa coefficient. The results indicate that our synthetic algorithm performed better than the pixel-based classification in ISA extraction.

Table 1. The confusion matrix by pixel-based classification

Reference / Algorithm Result	ISA	Non-ISA	Row Total	User's Accuracy %
ISA	42	8	50	84
Non-ISA	4	46	50	92
Column Total	46	54	100	0.76*
Producer's Accuracy %	91.3	85.2		88%**

*Kappa Value = 0.76
**Overall Accuracy = 88%

Table 2. The confusion matrix by synthetic algorithm

Reference / Algorithm Result	ISA	Non-ISA	Row Total	User's Accuracy %
ISA	46	4	50	92
Non-ISA	3	47	50	94
Column Total	49	51	100	0.86*
Producer's Accuracy %	93.9	92.2		93%**

*Kappa Value = 0.86
**Overall Accuracy = 93%

The results for the Rhode Island were evaluated as well (Fig. 5). With the same set of parameters, the ISA was extracted from the orthophoto using the synthetic algorithm and the results are visually satisfactory.

CONCLUSION AND DISCUSSION

This study developed a synthetic algorithm that includes submodels of segmentation, shadow-effect, maximum likelihood classification, and post-classification. A nested-hierarchical model approach was used in multiple pass algorithm. The segmentation submodel replaced the spectral difference with parameters of heterogeneity change for merging regions. The shape information was introduced in the segmentation submodel to enhance the performance of ISA extraction. In high spatial resolution images, particular in urban settings, it is unavoidable that some of the ISAs are covered by shadows of trees or buildings. Our shadow-effect submodel used a split-and-merge process to successfully separate shadows and the objects that cause the shadows. Through the maximum likelihood classifier, prior knowledge from available data sources could be integrated into the classification submodel for ISA identification. For those areas that are completely covered by dense tree crowns GIS based post-classification process enabled the recovery of the covered ISAs.

The results indicate that this synthetic algorithm performs better than the pixel-based classification in ISA extraction. The results of the state with different landscape and ISA characteristics prove that this algorithm is not a specialized method for the specific study area.

Compared with the pixel-based method, this synthetic algorithm can achieve more precise and accurate ISA distribution and eliminate the salt-and-pepper effect that is observable in the result from pixel-based method and the spatial information such as neighborhood, proximity and homogeneity is used sufficiently in the classification process. Furthermore, fewer training samples are needed for this algorithm since each sample region contains multiple pixel samples and their spectral variations.

Although our synthetic algorithm produces promising results for the ISA extraction from high spatial resolution imageries, further investigations will be conducted to improve this algorithm. First, the thresholds for the segmentation are important. The thresholds used in our experiment are derived from tests and perform well on all the study area. Second, comparative studies with existing program such as eCognition should be carried out. The comparison is important for the improvement of this synthetic algorithm. Third, the experiment using other high spatial resolution imageries such as IKONOS will be useful to test its extent of application.

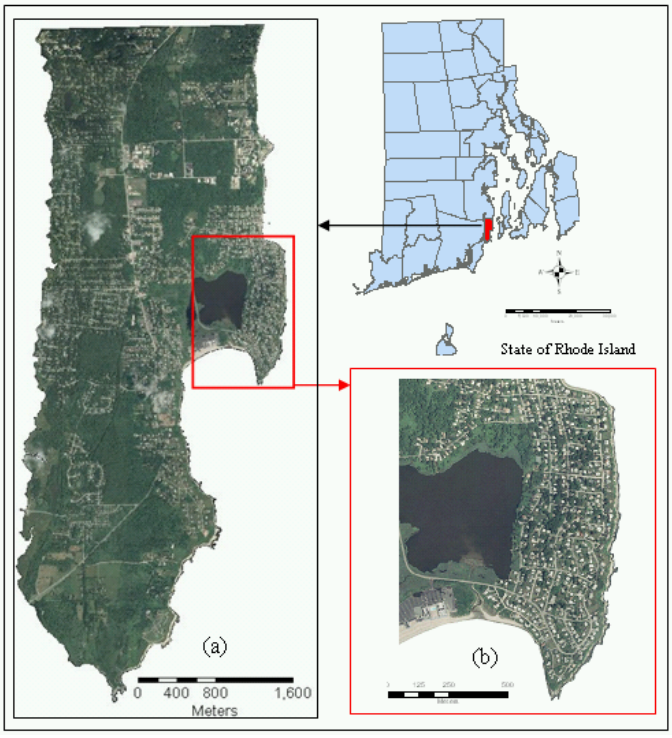

Figure 1. Study area of the state of Rhode Island for ISA extraction. a) Selected testing site of northern Narragansett, Rhode Island; b) an example of true-color digital orthophoto with 1-m spatial resolution.

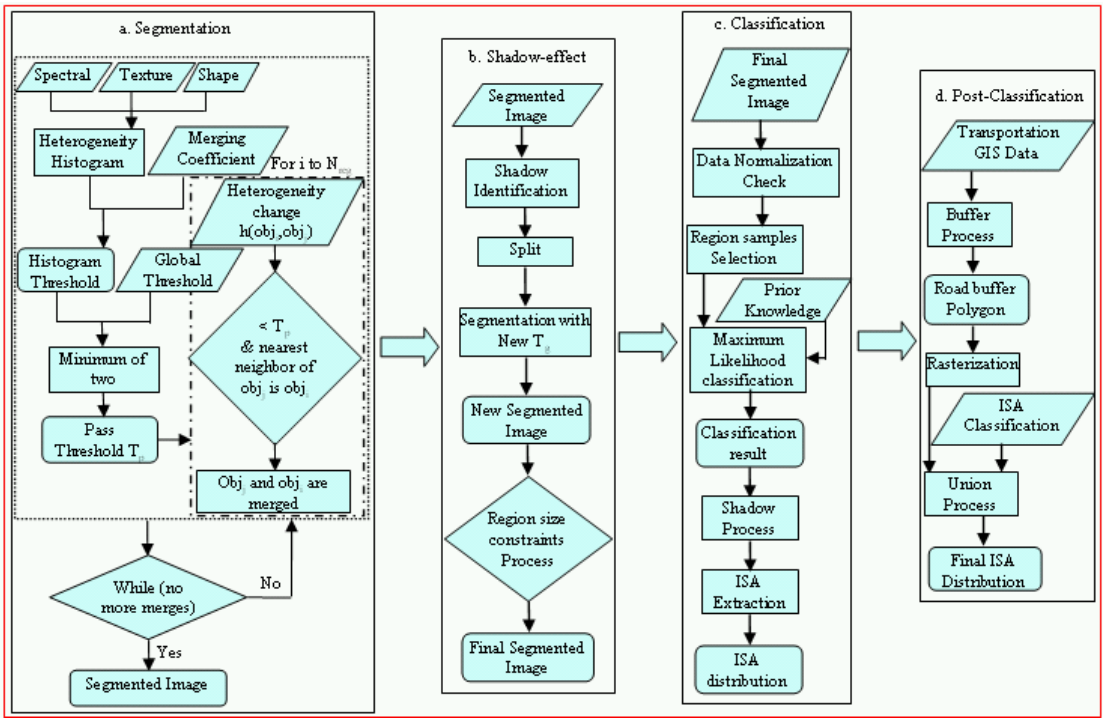

Figure 2. The flowchart of ISA extraction modeling. a) segmentation submodel; b) shadow-effect submodel; c) classification submodel based on segmented image; and d) post classification.

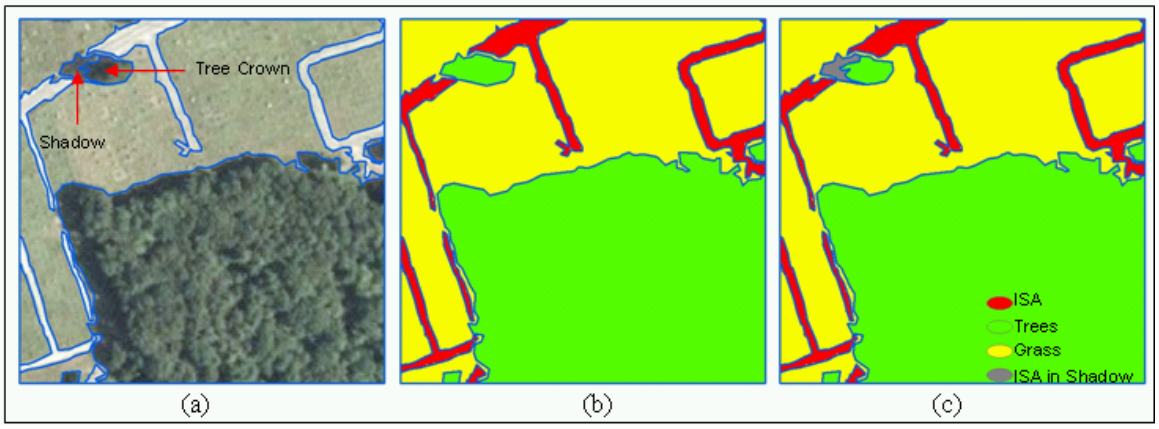

Figure 3. a) an example of spectral similarity of tree crowns and the shadow in a true color orthophoto; b) the result of image segmentation without considering the shadow effect, in which shadow covered ISA could not be separated from tree crowns that caused the shadows; c) the result of segmentation using the shadow-effect submodel.

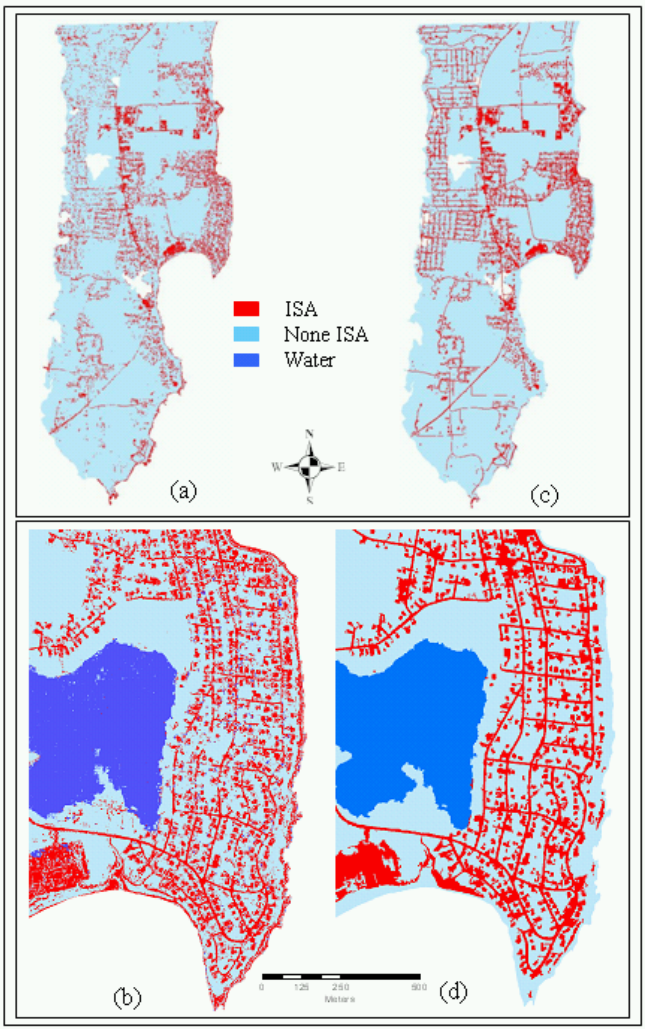

Figure 4. Extraction of ISA from pixel-based method ((a) and (b)); Extraction of ISA from synthetic algorithm ((c) and (d)).

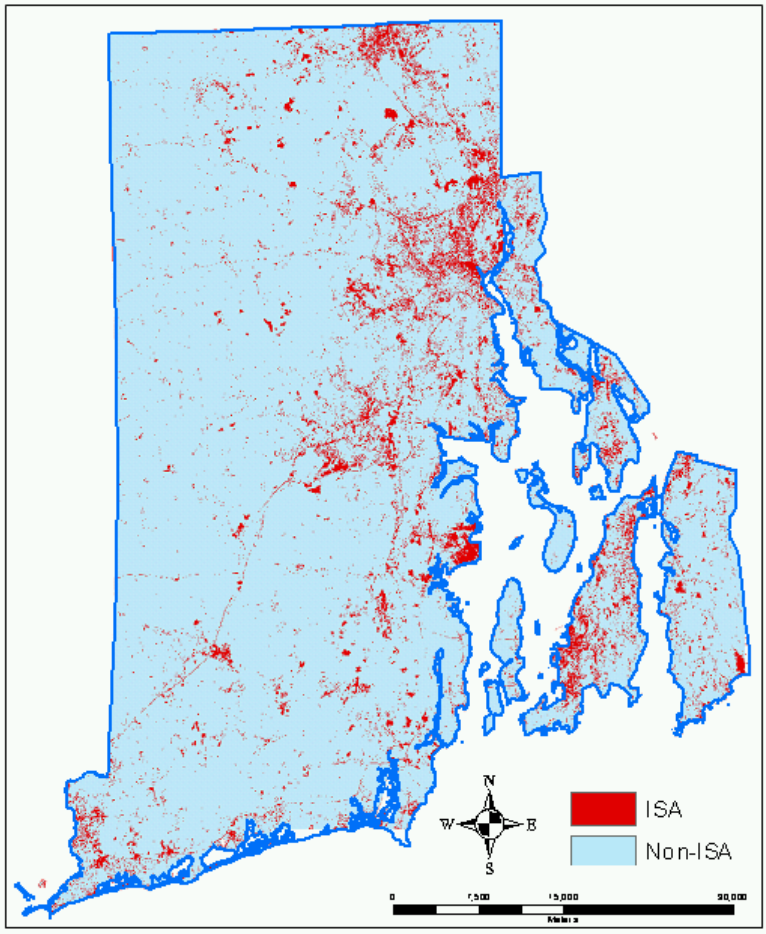

Figure 5. Extraction of ISA from the synthetic algorithm in Rhode Island.

ACKOWLEDGEMENTS

This project is funded by the Rhode Island Agricultural Experimental Station (Project No. H-330)

REFERENCES

Arnold, C.A. Jr., and C.J. Gibbons (1996). Impervious surface coverage: the emergence of a key urban environmental indicator. *Journal of the American Planning Association*, 62(2): 243-258.

Baatz, M. and A. Schäpe (2000). Multiresolution segmentation: an optimization approach for high quality multi-scale image segmentation, In: Strobl, J. and T. Blaschke (eds.): *Angewandte Geographische Informationsverarbeitung XII*. Wichmann-Verlag, Heidelberg, pp. 2-23.

Benz, U., P. Hofmann, G.. Willhauck, I. Lingenfelder, and M. Heynen (2004). Multi-resolution, object-oriented fuzzy analysis of remote sensing data for GIS-ready information. *ISPRS Journal of Photogrammetry & Remote Sensing*, 58 (3-4): 239– 258.

Blaschke, T., C. Burnett, and A. Pekkarinen (2004). New contextual approaches using image segmentation for object-based classification. In: De Meer, F. and S. de Jong (eds.): *Remote Sensing Image Analysis: Including the spatial domain*. Kluver Academic Publishers, Dordrecht, pp. 211-236.

Brabec, E., S. Schulte, and P. L. Richards (2002). Impervious Surfaces and Water Quality: A Review of Current Literature and Its Implications for Watershed Planning. *Journal of Planning Literature*, 16(4): 499-514.

Burnett, C., and T. Blaschke (2003). A multi-scale segmentation / object relationship modelling methodology for landscape analysis. Ecological Modelling, 168(3): 233-249.

Civco, D.L., J.D. Hurd, E.H. Wilson, C.L. Arnold, and S. Prisloe (2002). Quantifying and Describing Urbanizing Landscapes in the Northeast United States. *Photogrammetric Engineering & Remote Sensing*, 68(10): 1083-1090.

Comanicu, D., and P. Meer (2002). Mean shift: A robust approach toward feature space analysis. *IEEE Transactions on Pattern Analysis and Machine Intelligence*, 24(5): 603-619.

Dougherty, M., L. D. Randel, J. G.. Scott, A. J. Claire, and G. Normand (2004). Evaluation of Impervious Surface Estimates in a Rapidly Urbanizing Watershed. *Photogrammetric Engineering & Remote Sensing*, 70(11): 1275–1284.

Draper, S. E., and S. G., Rao (1986). Runoff Prediction Using Remote Sensing Imagery. *Water Resources Bulletin*, 22(6): 941-949.

Hay, G., T. Blaschke, D. Marceau, and A. Bouchard (2003). A comparison of three image-object methods for the multiscale analysis of landscape structure. *ISPRS Journal of Photogrammetry and Remote Sensing*, 57(5-6): 327-345.

Herold, M., A. Mueller, S. Guenter, and J. Scepan (2002). Object-oriented mapping and analysis of urban land use/cover using IKONOS data. *Proceedings of the 22nd EARSEL symposium*, 4-6 June 2002, Prague, Czech Republic (the European Association of Remote Sensing Laboratories), pp. 531-538.

Hu, X.Y., C.V. Tao, and P. Björn (2005). Automatic Segmentation of High Resolution Satellite Imagery by Integrating Texture, Intensity and Color Features. *Photogrammetric Engineering and Remote Sensing*, 71(12): 1399-1406.

Jennings, D., S.T. Jarnagin, and D. Ebert (2004). A modeling approach for determining watershed impervious surface area from National Land Cover Data 92. *Photogrammetric Engineering and Remote Sensing*, 70(11): 1295-1307.

Li, W., G. B. Benie, D.C. He, S.R. Wang, D. Ziou, Q. Gwyn, and J. Hugh (1999). Watershed-based hierarchical SAR image segmentation. *International Journal of Remote Sensing*, 20(17): 3378-3390.

Lu, D. and Q. Weng (2004). Spectral Mixture Analysis of the Urban Landscape in Indianapolis with Landsat ETM+ Imagery. *Photogrammetric Engineering & Remote Sensing*, 70(9): 1053-1062.

Meinel, G.., and M. Neubert (2004). A comparison of segmentation programs for high resolution remote sensing data. The International Archives of Photogrammetry, Remote Sensing and Spatial Information Sciences, Volume XXXV, Part B, Commission 4, 12-23 July, Istanbul, Turkey (International Society for Photogrammetry and Remote Sensing XXth Congress), unpaginated CD-ROM. 1097-1105, 2004

Novak, A. and Y. Wang (2004). Effects of Suburban Sprawl on Rhode Island's Forest: A Landsat View from 1972 to 1999. *Northeastern Naturalist*, 11(1): 67-74.

Shackelford, A.K and C. H. Davis (2003). A combined fuzzy pixel-based and object-based approach for classification of high-resolution multispectral data over urban areas. *IEEE Transactions on Geoscience & Remote Sensing*. 41(10): 2354-2363.

Sleavin, W.J., D.L. Civco, S. Prisloe, and L. Giannotti (2000). Measuring impervious surfaces for non-point source pollution modeling. *Proceedings of the ASPRS 2000 Annual Convention*, 22–26 May, Washington, D.C. (American Society for Photogrammetry and Remote Sensing, Bethesda, Maryland), unpaginated CD-ROM.

Walter, V. (2004). Object-based classification of remote sensing data for change detection. *ISPRS Journal of Photogrammetry & Remote Sensing*, 58: 225- 238.

Wang, L., W. P. Sousa, and P. Gong (2004). Integration of Object-based and Pixel-based Classification for Mapping Mangroves with IKONOS Imagery. *International Journal of Remote Sensing*, 25(1): 1-14.

Wang, Y. and X. Zhang (2004). A SPLIT Model for Extraction of Subpixel Impervious Surface Information. *Photogrammetric Engineering and Remote Sensing*, 70(7): 821-828.

Weng, Q. H (2001). Modeling Urban Growth Effects on Surface Runoff with the Integration of Remote Sensing and GIS. *Environmental Management*, 28(6): 737-748.

Woodcock, C. E., and V. J. Harward (1992). Nested-Hierarchical Scene Models and Image Segmentation. *International Journal of Remote Sensing*, 13(16): 3167-3187.